Suppemental Fig. S1

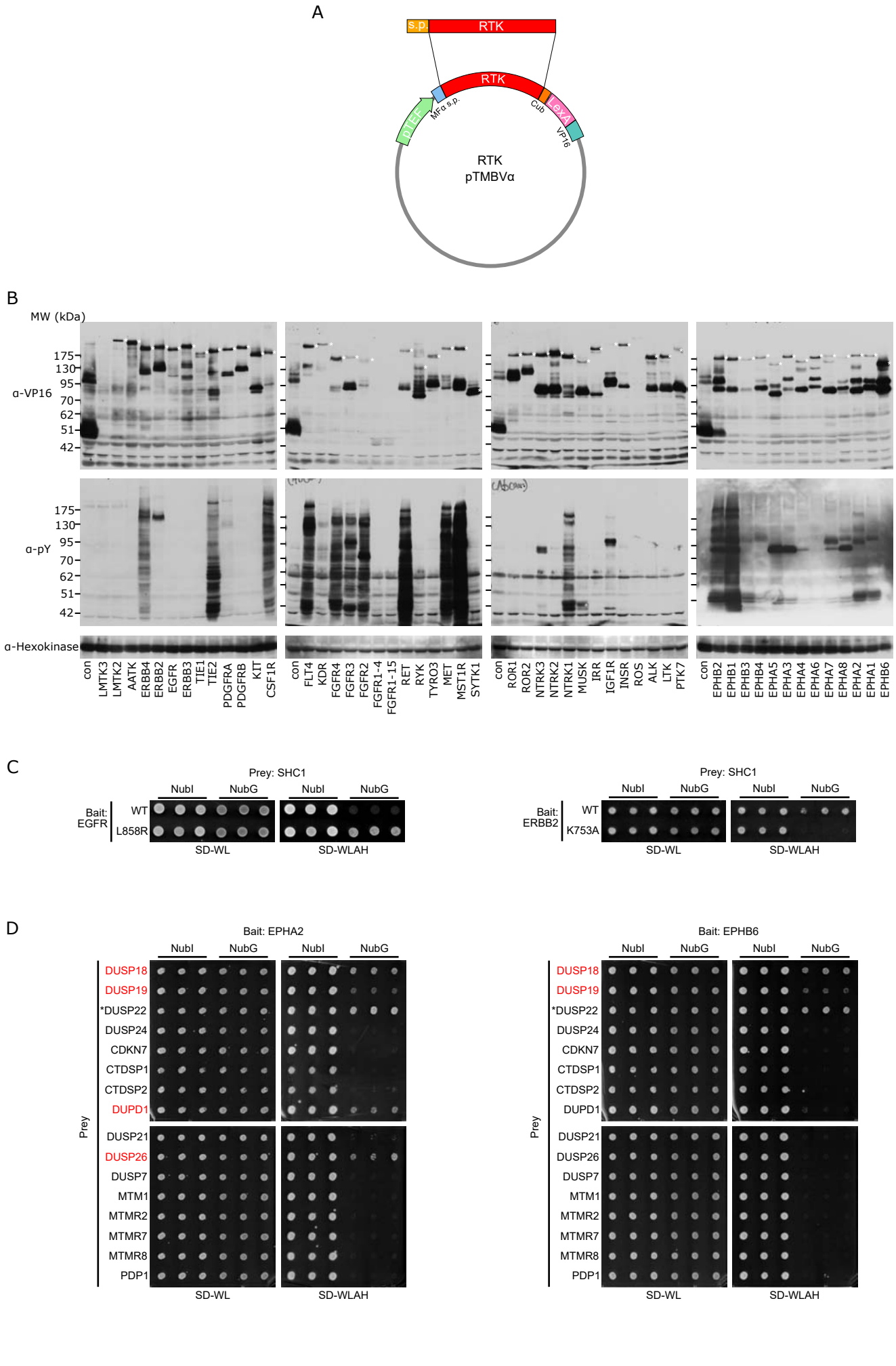

Supplemental Fig. S2

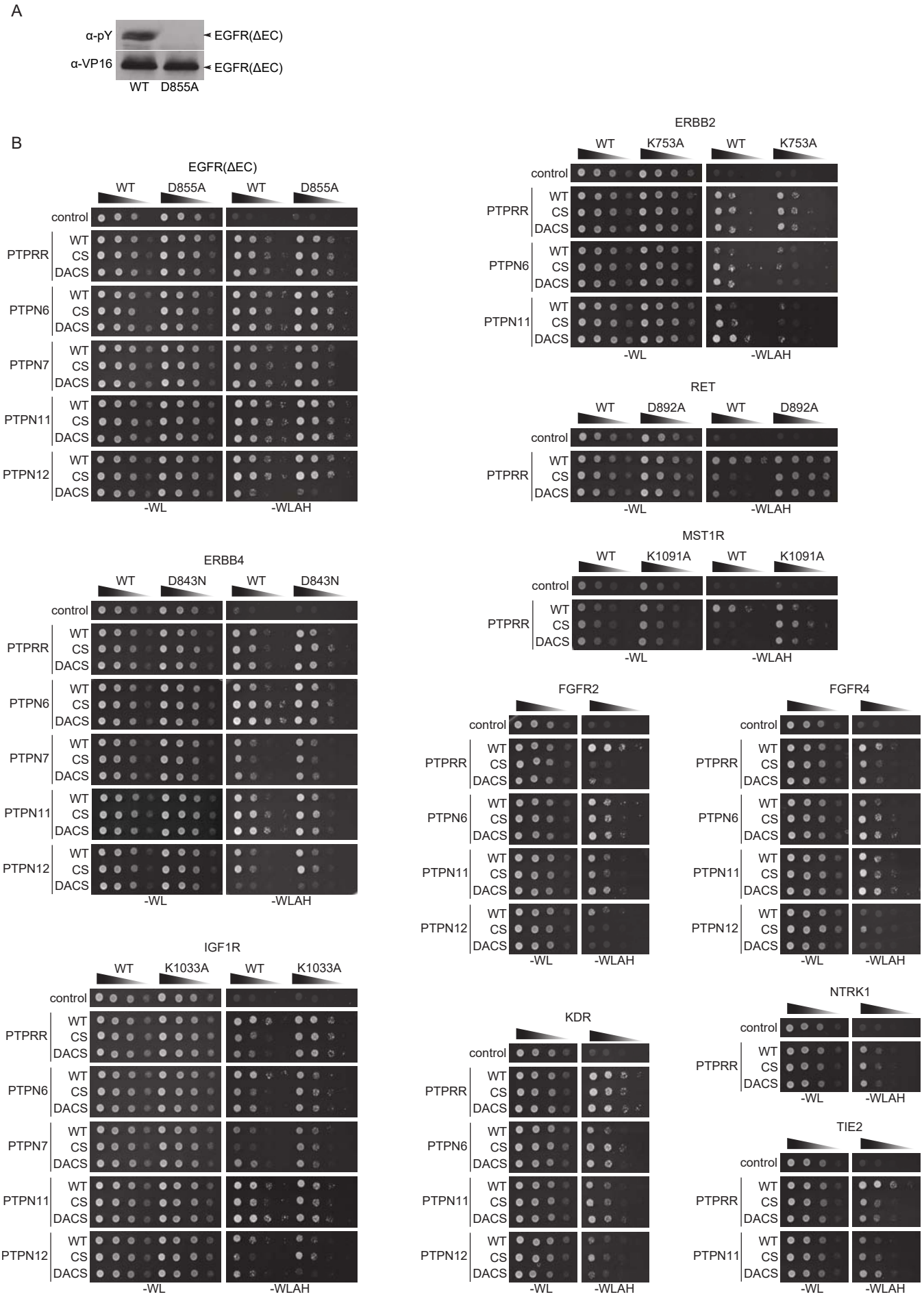

Supplemental Fig. S3

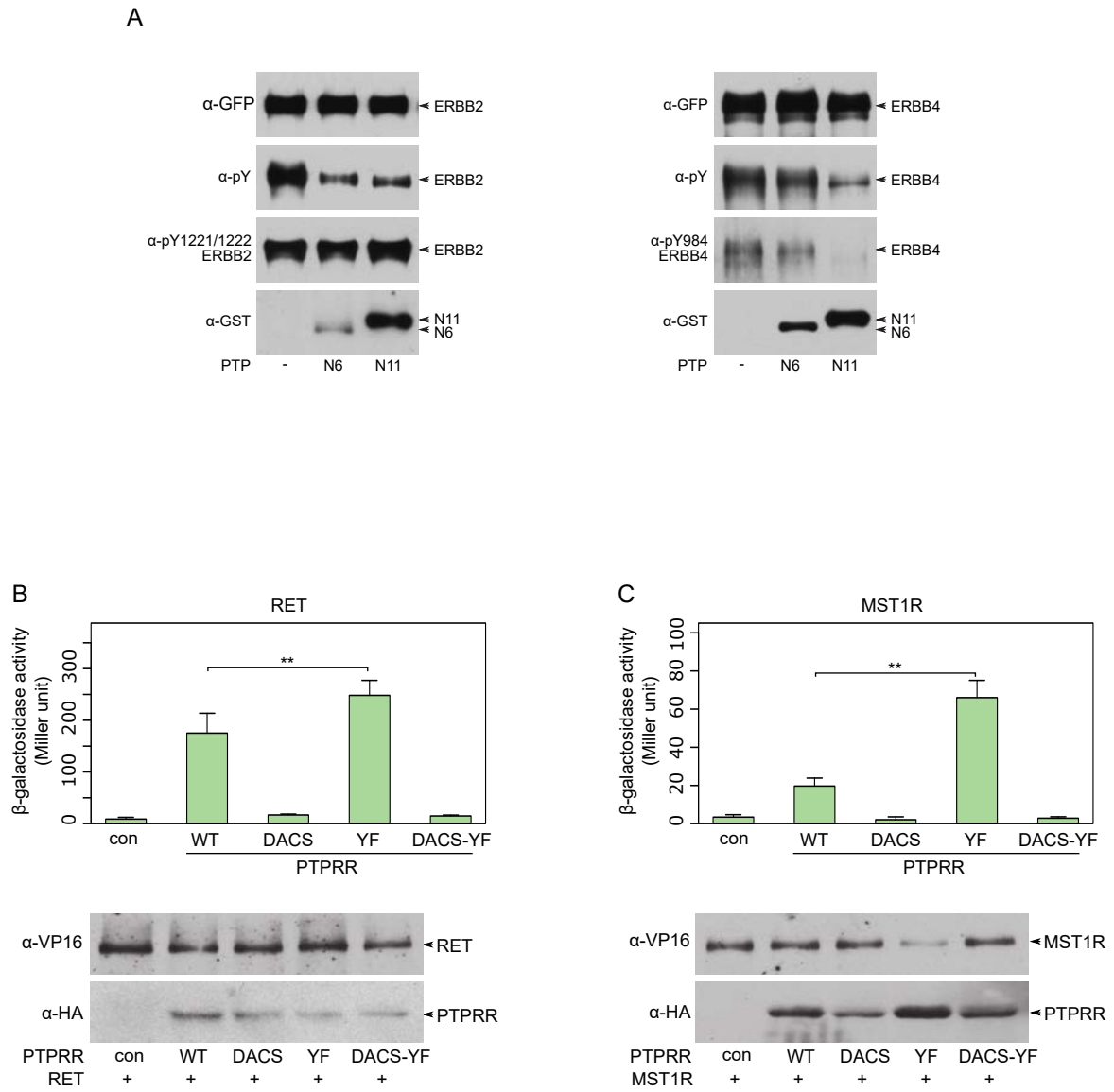

Supplementary Fig. S4

A

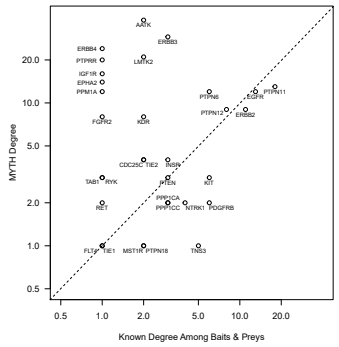

B

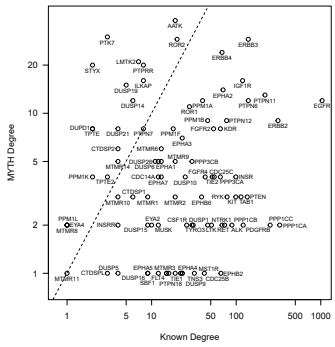

E

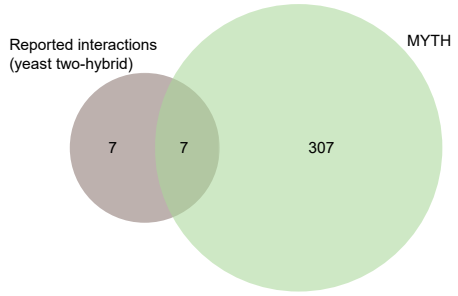

C

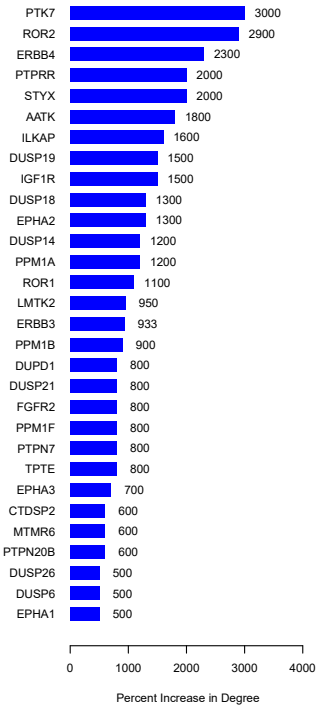

D

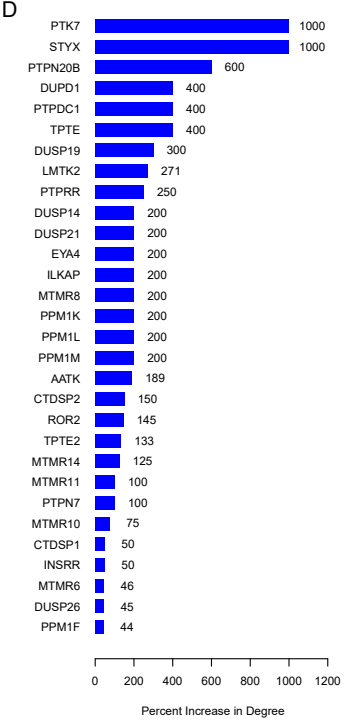

F

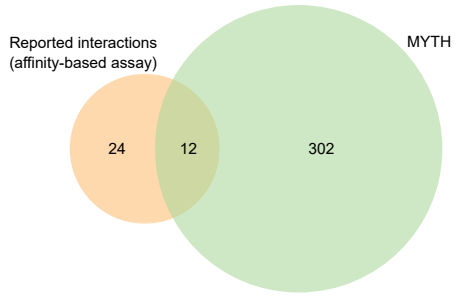

G

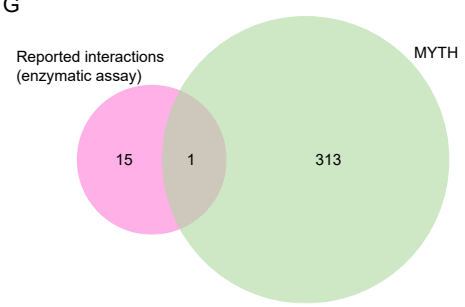

Supplemental Fig. S5

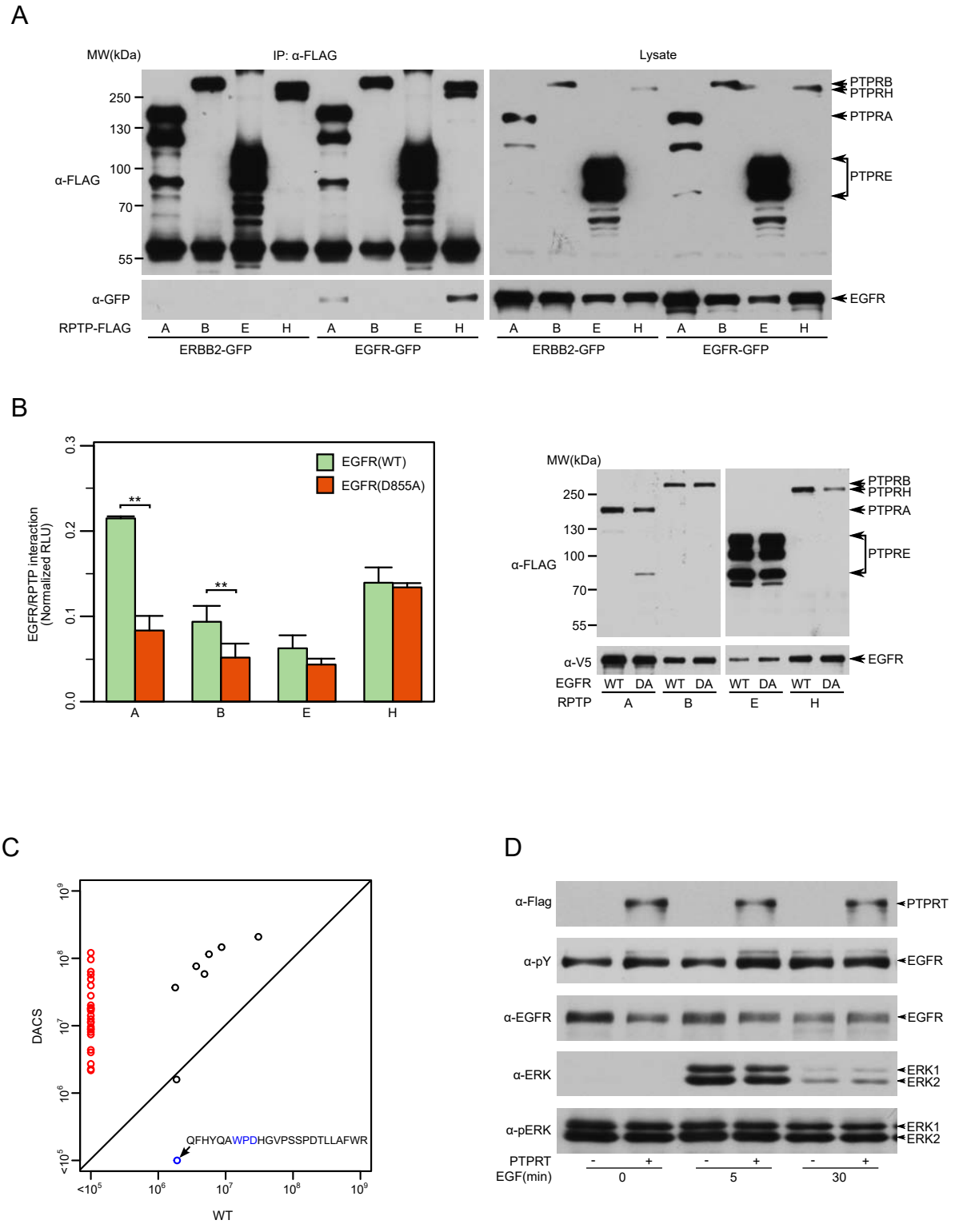

Supplemental Fig. S6

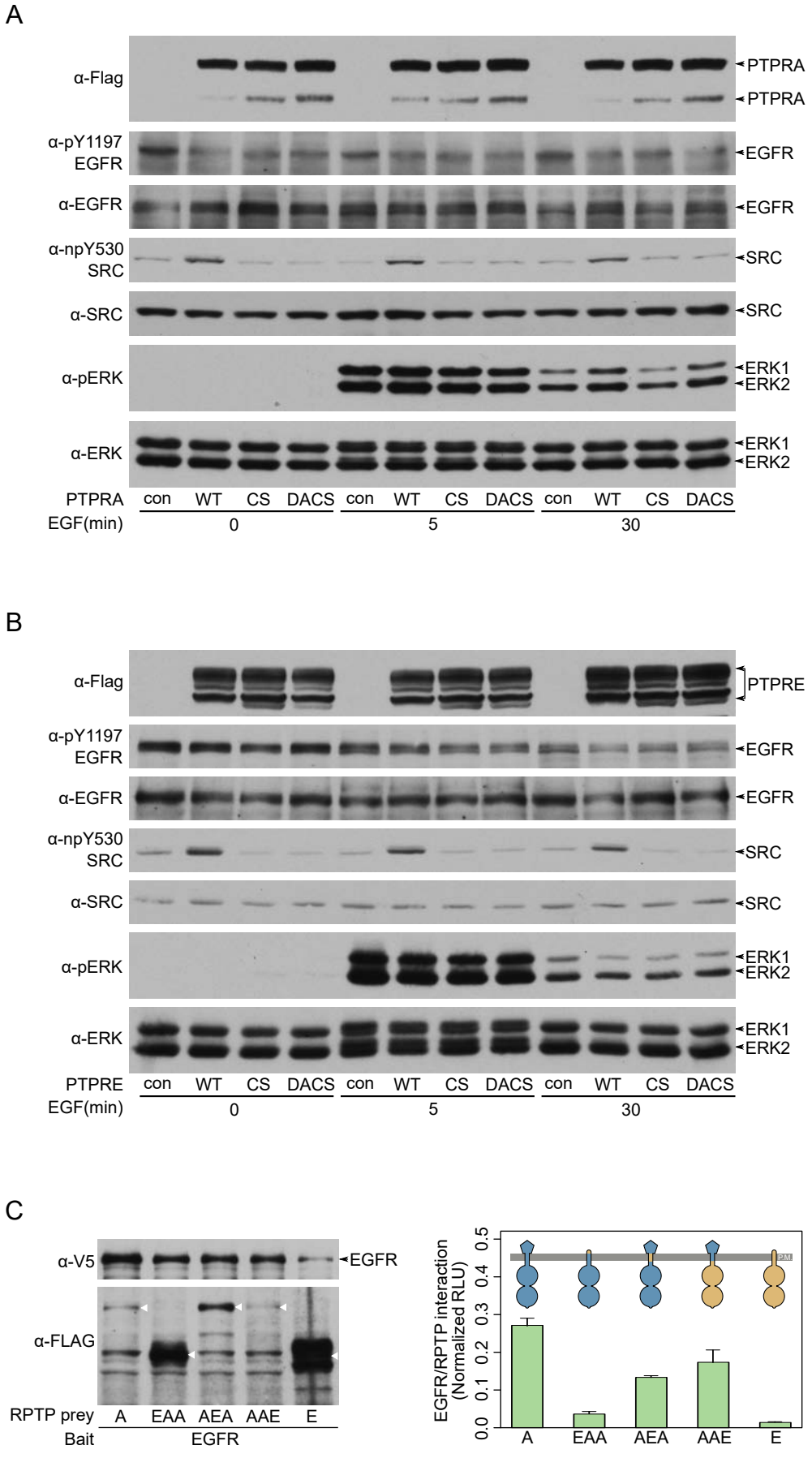

LEGENDS FOR SUPPLEMENTAL FIGURES

Figure S1. Related to Figure 1. RTK bait preparation for MYTH assay and MYTH screen.
A. RTK ORFs were cloned into a MYTH bait vector (pTMBVα) with their native signal peptide sequence (s.p.) replaced by mating factor α signal peptide (MFα s.p.).
B. Validation of RTK expression in yeast cells by Western blotting with α-VP16 antibodies. RTK activity state was detected by blotting with anti-general phosphotyrosine antibody PY99. Two alternatively spliced forms of FGFR1, isoform 4 (FGFR1-4) and isoform 15 (FGFR1-15), were tested in study.
C. Functional characterization of RTK baits by MYTH assay. EGFR (left), either WT (inactive when expressed in yeast) or active mutant L858R, and ERBB2 (right), either WT (constitutively active when expressed in yeast) or inactive mutant K753A, were tested against SHC1.
D. Example MYTH screens. Shown here are final results of yeast growth on selective medium (SD-WLAH) using example baits EPHA2 (left) or EPHB6 (right). Growth on non-selective medium (SD-WL) and NubI version of preys were used as controls. Positive interactions are highlighted by red color and frequent flyer is labelled with "*".

Figure S2. Related to Figure 2. MYTH assays describing PPIs between RTKs and PTP mutants.
A. Constitutively active EGFR was generated by deleting the extracellular region (ΔEC) for further MYTH assay. Activity of this construct was assessed by immunoblotting using α-pTyr (PY99) antibody. Note that activity is abolished by mutating the key kinase domain residue Asp855 to alanine.
B. The relative strength of interactions between RTKs and PTP mutants was assessed by growth of serially diluted yeast cells on selective medium (SD-WLAH). EGFR ΔEC D855A, ERBB2 K753A, ERBB4 D843A, IGF1R K1033A, RET D892A and K1091A are inactive RTK mutants.

Figure S3. Related to Figure 2. Functional characterization of RTK/phosphatase interactions.
A. In vitro phosphatase assay. GFP-tagged ERBB2 or ERBB4 were expressed in cells. The proteins were phsophorylated through pervanadate treatment and were pulled down by α-GFP antibody. Phosphatase activities were assessed by incubating recombinant PTPN6 or PTPN11 with immunoprecipitated ERBB2 (left) or ERBB4 (right), followed by Western blot analysis with anti-phosphotyrosine antibodies.
B-C. Tyr249 plays a role in PTPRR-RTK interaction. MYTH assay using either RET (B) or MST1R (C) as bait was performed against PTPRR WT or PTPRR mutants. DACS: Asp554Ala and Cys588Ser mutant; YF: Y249F mutant; DACS-YF: Y249F, D554A and C588S triple mutant. ONPG assays were used as the readout. Data represent mean ± SD (n=6). Significance was assessed by one-tailed Student's t-test. **: $P<0.01$. The expression level of each bait or prey was determined by immunoblotting using anti-tag antibodies, VP16 for bait and HA for prey.

Figure S4. Related to Figure 4. Comparison of RTK-phosphatase interactome revealed by MYTH with reported PPIs.
A. Degrees of RTKs and phosphatases in results from MYTH compared to a network comprising previously known interactions among these proteins. Degree is defined as the number of interacting partners of a protein. Degrees are plotted using a log-log scale. A dashed line indicates equal *x,y* values.
B. Degrees of RTKs and phosphatases in results from MYTH and the known human interactome. Degrees are plotted using a log-log scale. A dashed line indicates equal *x,y* values. Log-log plot showing degrees of RTKs and phosphatases from MYTH versus their degrees in the known human interactome.
C. Increases in protein degree in the network of tested RTK-phosphatase pairs, due to the MYTH screen. Shown are proteins with the top 30 percentage increases in degree.
D. Increases of protein degree in the known human interactome, due to the MYTH screen. Shown are proteins with the top 30 percentage increases in degree.
E-G. Comparison of RTK-phosphatase interactome revealed by MYTH with reported interactions obtained by different methods. Reported RTK-phosphatase interactions (Fig. 4A) were categorized according to the methods used: yeast two-hybrid (E), affinity-based (including affinity chromatography, co-immunoprecipitation, pull-down assay and tandem affinity purification) (F) and enzymatic assays (G). Each category is compared with the interactome obtained by MYTH using a Venn diagram.

Figure S5. Related to Figure 5.

A. GFP-tagged EGFR or ERBB2, together with FLAG-tagged PTPRA, PTPRB, PTPRE or PTPRH were co-transfected into HEK 293 cells. The cells were lysed with a buffer containing 0.3% CHAPS and 0.07% Triton X-100. Related proteins were immunoprecipitated by α–FLAG antibody and the co-precipitated EGFR or ERBB2 were probed with α-GFP antibody.
B. Effects of EGFR activity on EGFR/RPTP interactions. MaMTH assay was performed with EGFR WT or inactive mutant (D855A) as baits and PTPRA, PTPRB, PTPRE or PTPRH as preys. The values were normalized with the signal obtained from EGFR/SHC1 interaction in the same experiment. Data represent mean ± SD (n=3). Significance was assessed by two-tailed Student's t-test. **: $P<0.01$. The expression level of the proteins is shown by Western blot analysis in the right panel.
C. PTPRH trapping mutant interacts with EGFR. EGFR-GFP was cotransfected into HEK293 cells with PTPRH (WT or DACS mutant). After 5 minutes of EGF stimulation (100 ng/ml), EGFR-GFP was immunoprecipitated by α-GFP antibody followed by MS analysis. PTPRH was co-precipitated with EGFR as judged by MS. The intensities of PTPRH peptides from the DACS mutant were plotted against those from WT using a scatter plot. Peptides detected only in DACS immunoprecipitates, not in WT are highlighted in red. The only peptide detected solely in WT immunoprecipitates was the WPD motif peptide (highlighted in blue) which is altered in the DACS mutant.
D. PTPRT does not have a marked effect on EGFR signaling. HEK293 cells were transfected with PTPRT. The cells were stimulated with EGF followed by Western blotting with the indicated antibodies.

Figure S6. Related to Figure 6.
A. Effects of PTPRA mutants on EGFR signaling. WT, CS or DACS mutant was transfected into HEK 293 cells. After EGF stimulation for the indicated periods of time, the cells were lysed and the lysates were subject to Western blot analysis with the indicated antibodies.
B. PTPRE and its inactive mutants did not have significant effects on EGFR signaling. Similar to (A) except using PTPRE and the corresponding mutants.
C. Mapping domains responsible for PTPRA/EGFR interaction. The extracellular region (EAA), the transmembrane domain (AEA) and the intracellular part (AAE) of PTPRA was substituted with their counterparts in PTPRE, respectively, as indicated in the inset of the right panel. The MaMTH assay was performed using EGFR as bait, and the chimera PTPRA/E proteins, as well as WT PTPRA and PTPRE, as preys. Data represent mean ± SD (n=3). The expression of different proteins is shown in the left panel.

SUPPLEMENTAL TABLE

Table S1. Related to Figure 5.

SUPPLEMENTAL EXPERIMENTAL PROCEDURES

Molecular cloning and library preparation

Most cDNAs were originally obtained from human ORFeome collection or from the Openfreezer collection at Lunenfeld-Tanenbaum Research Institute (Olhovsky et al., 2011). Those not in entry clone vectors were cloned into pDONR223 by PCR and Gateway BP reactions (Life Technologies). For MYTH assays, the cDNAs were cloned into the pGPR3N (NubG or NubI for control) prey vector by Gateway LR cloning (Life Technologies). RTK cDNAs were cloned into the pTMBVα bait vector by PCR and gap-repair with their own signal peptide sequences replaced by MFα signal sequence. For MaMTH assays, RTK cDNAs were cloned into the pV1900Cub-Gal4-RelA-V5 bait vector by LR cloning, and the RPTP cDNAs were cloned into pV1900Nub-Flag prey vector by LR cloning. Site-directed mutagenesis was generated by PCR using KAPA HiFi DNA polymerase (KAPA Biosystems).

Cell culture and treatment

HEK293T MaMTH reporter cells or HEK293 cells were grown in DMEM supplemented with 10% fetal calf serum (Gibco). Cells were transfected with various plasmids by PolyJet (SignaGen Laboratories) or calcium phosphate precipitation. The transfected cells were serum-starved (0.1% FCS) overnight, and then treated with 100ng/ml EGF (Sigma) for 0 to 30 minutes. In some experiments, the cells were pretreated with different inhibitors for 30 min before EGF stimulation. OV-90 cells were maintained in ovarian surface epithelium (OSE) complete medium supplemented with 10% fetal calf serum and were transfected by TransIT-X2 (Mirus Bio LLC).

Western blot analysis and immunoprecipitation

Yeast proteins were extracted as described (Yaffe and Schatz, 1984). Mammalian cells were lysed in buffer H (Triton X 100 1%, β-glycerophosphate pH7.3 50 mM, EGTA 1.5 mM, EDTA 1 mM, orthovanadate 0.1 mM, DTT 1 mM supplemented with protease inhibitors (Roche)). After centrifugation at 15,000 rpm for 10 min, the supernatants were mixed with Laemmli sample buffer, boiled at 95 ^{0}C for 3-5 min and subject to Western blot analysis. For immunoprecipitations, supernatants (0.3 ml) were incubated with antibodies at 4^{o}C with rotating for one hour, followed by another hour of incubation with protein G sepharose beads (GE Healthcare). Beads were washed twice with LiCl (0.5 M in Tris pH8.0 0.1 mM) and twice with lysis buffer, and then subjected to MS analysis. Co-immmunoprecipitation was performed first by treating the cells with 0.5 mM dithiobis succinimidyl propionate (Thermo Fisher) at room temperature for 30 min followed by quenching with a buffer containing 0.1 M pH 7.5 Tris-HCl and EDTA 2 mM. The cells were lysed with RIPA buffer and the proteins were precipitated with corresponding antibodies with wash by RIPA buffer. Alternative co-immunoprecipitation was performed using a lysis buffer containing 50mM pH7.5 Tris-HCl, NaCl 120 mM, EDTA 1 mM, β-glycerophosphate 10 mM, orthovanadate 0.1 mM, 0.3% CHAPS and 0.7% Triton-X 100. Antibodies used for Western blot analysis and immunoprecipitations were: α-VP16, α-Flag antibodies were purchased from Sigma-Aldrich Co., α-HA, and α-GFP antibodies were from Roche Diagnostics, α-pY (PY99), α-pY1197 EGFR and α-ERK1/2 antibodies were from Santa Cruz Biotechnology, α-EGFR, α-pERK, α-npY530 SRC, α-SRC, and α-V5 antibodies were from Cell Signaling Technology, α-PTPRH antibodies were from Pierce. Each of the above antibodies was diluted according to provider's protocol. For immunoprecipitation, 2 μg α-GFP antibody was used for each sample.

***In vitro* PTP assay**

Recombinant PTPN6 and PTPN11 and their activity assay were performed as described (O'Reilly et al., 2000). The substrates, ERBB2 and ERBB4, were prepared by expressing the GFP-tagged proteins in HEK 293T cells and treating the cells with pervanadate for 15 min followed by immunoprecipitation with α-GFP antibody.

***PTPRH* deletion by CRISPR/Cas9**

A guide sequence, TGTTGGGTCTCGGGCCGGCT, was chosen to target the PTPRH gene and was cloned into vector pX330. This plasmid was transfected into OV-90 cells, and single clones were obtained after cell sorting. Properly deleted clones were verified by Western blot analysis using α-PTPRH antibodies.

Comparisons with previously known interactions of RTKs and protein phosphatases

Previously known interactions of RTKs and protein phosphatases were obtained from IID ver. 2015-09 (http://www.cs.utoronto.ca/iid) (Kotlyar et al., 2016), which integrates data from multiple sources, including 7 major PPI databases: BioGRID (http://thebiogrid.org/) (Chatr-Aryamontri et al., 2015) 3.4.125, DIP (http://dip.doe-mbi.ucla.edu/dip/Main.cgi) (Salwinski et al., 2004) 2015-01-01, HPRD (http://www.hprd.org/) (Keshava Prasad et al., 2009) Release 9, I2D (http://ophid.utoronto.ca/ophidv2.204/) (Brown and Jurisica, 2007) 2.3, InnateDB (http://www.innatedb.ca/) (Breuer et al., 2013) 2015-05-23, IntAct (http://www.innatedb.ca/) (Kerrien et al., 2012) 2015-06-13, and MINT (http://mint.bio.uniroma2.it/mint/Welcome.do) (Licata et al., 2012) 2013-03-26. Data processing and visualization was done using Perl 5.14.2, R 3.1.2, and NAViGaTOR (Brown et al., 2009) ver. 2.3 (http://ophid.utoronto.ca/navigator).

Mass spectrometry

Mass spectrometry analysis was performed as described (Guo et al., 2013). Briefly, the protein was reduced by DTT, alkylated by iodoacetamide and further digested by trypsin over night. Digested samples were dried and re-suspended in 200μL 80% acetonitrile/2% formic acid, followed by mixing with TiO_2 coated magnetic beads (Pierce) to enrich for phosphopeptides. Binding buffer and washing buffer (supplied by the manufacturer) were used to wash the beads. Finally, the phosphopeptides were eluted using elution buffer and dried. The peptides were injected into C18 nano-column on an EASY-nLC (Proxeon) coupled to an Orbitrap Velos mass spectrometer (Thermo Fisher Scientific). A 90 min gradient was used for separation at a flow rate of 300nL/minutes. Sixteen MS/MS collision-induced dissociation (CID) data-dependent scans were acquired simultaneously with one full scan mass spectra with 60000 resolution and 1E6 AGC. MaxQuant (version 1.5.1.0) was used to search Uniprot/SwissProt human protein database with 22,491 human proteins modified to contain BSA and trypsin, with variable modification of methionine oxidation, protein N-terminal acetylation and phosphorylation of serine/threonine/tyrosine specified as variable modifications and with cysteine carbamidomethylation as a fixed modification. A 1% false discovery rate threshold was applied for both peptides and proteins. All tyrosine-phosphorylated peptides were validated manually. The mass spectrometry proteomics data have been deposited to the ProteomeXchange Consortium via the PRIDE (Vizcaíno et al., 2016) partner repository with the dataset identifier PXD004248.

SUPPLEMENTAL REFERENCES

Breuer, K., Foroushani, A.K., Laird, M.R., Chen, C., Sribnaia, A., Lo, R., Winsor, G.L., Hancock, R.E.W., Brinkman, F.S.L., Lynn, D.J., 2013. InnateDB: Systems biology of innate immunity and beyond - Recent updates and continuing curation. Nucleic Acids Res. 41, 1228–1233.

Brown, K.R., Jurisica, I., 2007. Unequal evolutionary conservation of human protein interactions in interologous networks. Genome Biol 8, R95.

Brown, K.R., Otasek, D., Ali, M., McGuffin, M.J., Xie, W., Devani, B., Toch, I.L. van, Jurisica, I., 2009. NAViGaTOR: Network Analysis, Visualization and Graphing Toronto. Bioinformatics 25, 3327–9.

Chatr-Aryamontri, A., Breitkreutz, B.-J., Oughtred, R., Boucher, L., Heinicke, S., Chen, D., Stark, C., Breitkreutz, A., Kolas, N., O'Donnell, L., Reguly, T., Nixon, J., Ramage, L., Winter, A., Sellam, A., Chang, C., Hirschman, J., Theesfeld, C., Rust, J., Livstone, M.S., Dolinski, K., Tyers, M., 2015. The BioGRID interaction database: 2015 update. Nucleic Acids Res. 43, D470-478.

Guo, H., Isserlin, R., Chen, X., Wang, W., Phanse, S., Zandstra, P.W., Paddison, P.J., Emili, A., 2013. Integrative network analysis of signaling in human CD34+ hematopoietic progenitor cells by global phosphoproteomic profiling using TiO2 enrichment combined with 2D LC-MS/MS and pathway mapping. Proteomics 13, 1325–1333.

Kerrien, S., Aranda, B., Breuza, L., Bridge, A., Broackes-Carter, F., Chen, C., Duesbury, M., Dumousseau, M., Feuermann, M., Hinz, U., Jandrasits, C., Jimenez, R.C., Khadake, J., Mahadevan, U., Masson, P., Pedruzzi, I., Pfeiffenberger, E., Porras, P., Raghunath, A., Roechert, B., Orchard, S., Hermjakob, H., 2012. The IntAct molecular interaction database in 2012. Nucleic Acids Res. 40, D841-846.

Keshava Prasad, T.S., Goel, R., Kandasamy, K., Keerthikumar, S., Kumar, S., Mathivanan, S., Telikicherla, D., Raju, R., Shafreen, B., Venugopal, A., Balakrishnan, L., Marimuthu, A., Banerjee, S., Somanathan, D.S., Sebastian, A., Rani, S., Ray, S., Harrys Kishore, C.J., Kanth, S., Ahmed, M., Kashyap, M.K., Mohmood, R., Ramachandra, Y.L., Krishna, V., Rahiman, B.A., Mohan, S., Ranganathan, P., Ramabadran, S., Chaerkady, R., Pandey, A., 2009. Human Protein Reference Database--2009 update. Nucleic Acids Res 37, D767-772.

Kotlyar, M., Pastrello, C., Sheahan, N., Jurisica, I., 2016. Integrated interactions database: tissue-specific view of the human and model organism interactomes. Nucleic Acids Res. 44, D536-541.

Licata, L., Briganti, L., Peluso, D., Perfetto, L., Iannuccelli, M., Galeota, E., Sacco, F., Palma, A., Nardozza, A.P., Santonico, E., Castagnoli, L., Cesareni, G., 2012. MINT, the molecular interaction database: 2012 update. Nucleic Acids Res. 40, D857-861.

O'Reilly, A.M., Pluskey, S., Shoelson, S.E., Neel, B.G., 2000. Activated mutants of SHP-2 preferentially induce elongation of Xenopus animal caps. Mol. Cell. Biol. 20, 299–311.

Olhovsky, M., Williton, K., Dai, A.Y., Pasculescu, A., Lee, J.P., Goudreault, M., Wells, C.D., Park, J.G., Gingras, A.-C., Linding, R., Pawson, T., Colwill, K., 2011. OpenFreezer: a reagent information management software system. Nat. Methods 8, 612–613.

Salwinski, L., Miller, C.S., Smith, A.J., Pettit, F.K., Bowie, J.U., Eisenberg, D., 2004. The Database of Interacting Proteins: 2004 update. Nucleic Acids Res 32, D449-451.

Vizcaíno, J.A., Csordas, A., Del-Toro, N., Dianes, J.A., Griss, J., Lavidas, I., Mayer, G., Perez-Riverol, Y., Reisinger, F., Ternent, T., Xu, Q.-W., Wang, R., Hermjakob, H., 2016. 2016 update of the PRIDE database and its related tools. Nucleic Acids Res. 44, D447-456.

Yaffe, M.P., Schatz, G., 1984. Two nuclear mutations that block mitochondrial protein import in yeast. Proc. Natl. Acad. Sci. U. S. A. 81, 4819–4823.